



Near-term regional climate change in East Africa

Yeon-Woo Choi¹ · Deborah J. Campbell² · Elfatih A.B. Eltahir¹

Received: 4 April 2022 / Accepted: 8 November 2022 / Published online: 24 November 2022
© The Author(s) 2022, corrected publication 2023

Abstract

In the coming few decades, projected increases in global temperature and humidity are generally expected to exacerbate human exposure to climate extremes (e.g., humid-heat and rainfall extremes). Despite the growing risk of humid-heat stress (measured by wet-bulb temperature), it has received less attention in East Africa, where arid and semi-arid climatic conditions prevail. Moreover, no consensus has yet been reached across models regarding future changes in rainfall over this region. Here, we screen Global Climate Models (GCMs) from CMIP5 and CMIP6 and use, for boundary conditions, simulations from only those GCMs that simulate successfully recent climatic trends. Based on these GCMs and Regional Climate Model (RCM) simulations, we project that annual mean temperature is likely to rise by 2 °C toward midcentury (2021–2050) at a faster rate than the global average (about 1.5 °C), under the RCP8.5 and SSP5-8.5 scenarios, associated with more frequent and severe climate extremes. In particular, low-lying regions in East Africa will be vulnerable to severe heat stress, with an extreme wet-bulb temperature approaching or exceeding the US National Weather Service’s extreme danger threshold of 31 °C. On the other hand, population centers in the highlands of Ethiopia will receive significantly more precipitation during the autumn season and will see more extreme rainfall events, with implications for flooding and agriculture. The robustness of these results across all GCM and RCM simulations, and for both of CMIP5 and CMIP6 frameworks (CMIP: Coupled Model Inter-comparison Project) supports the reliability of these future projections. Our simulations of near-term climate change impacts are designed to inform the development of sound adaptation strategies for the region.

Keywords Regional climate model · Fine-scale climate projections · Extreme precipitation · Heat stress · East Africa

1 Introduction

With global warming accelerating, climate extremes, such as heatwaves and heavy rainfall, have attracted much attention in past decades due to their impacts on natural and human systems (Meehl and Tebaldi 2004; Kharin et al. 2013; Sillmann et al. 2013; Fischer and Knutti 2015). The risks from climate change vary significantly depending on

geographical location, selected period, and adaptive capacity by country (IPCC 2013). Developing countries in East Africa are particularly vulnerable to climate change impacts because of their limited resources, strong dependence on rain-fed agriculture, and high level of water scarcity (Niang et al. 2014; Kruger 2018; Allam and Eltahir 2019; Eltahir et al. 2019). Climate change is already a reality in this region (Russo et al. 2016; Herold et al. 2017; Nangombe et al. 2018; Gebrechorkos et al. 2019; WMO 2020). Further warming is probably unavoidable due to the persistent increase in greenhouse gas concentrations at or above the current rates (e.g., Niang et al. 2014).

Long-term climate records indicate rapid warming in East Africa at a faster rate than the global mean (Engelbrecht et al. 2015; WMO 2020), resulting in more frequent, more intense, and longer-lasting heatwaves (Engelbrecht et al. 2015; Russo et al. 2016; Herold et al. 2017; Nashwan and Shahid 2019). The Nile basin countries, including Sudan and Ethiopia (hereafter referred to as East Africa; Fig. 1), are

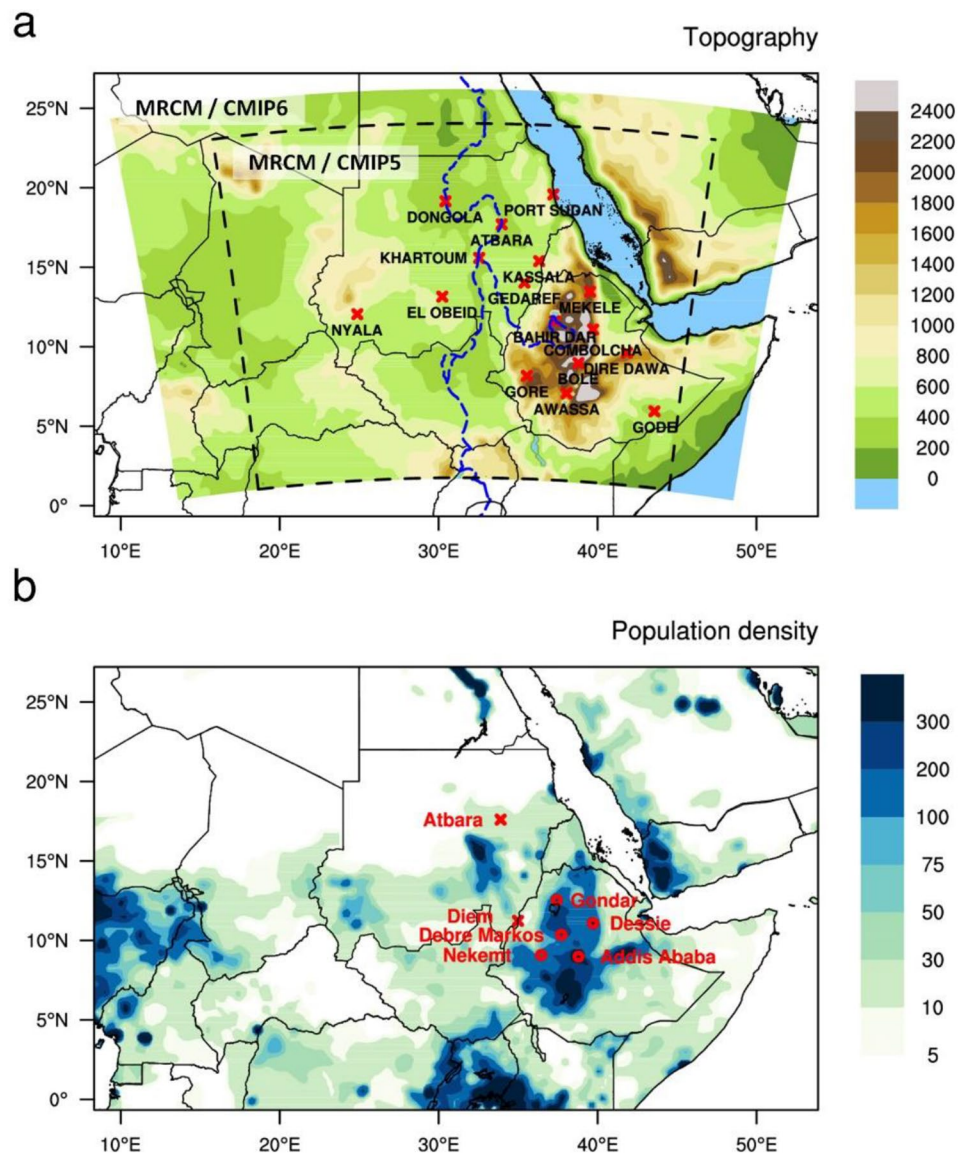
The original online version of this article was revised: In this article some text was changed under the section Funding and acknowledgement.

✉ Elfatih A.B. Eltahir
eltahir@mit.edu

¹ Ralph M. Parsons Laboratory, Massachusetts Institute of Technology, 02139 Cambridge, MA, USA

² Lincoln Laboratory, Massachusetts Institute of Technology, Cambridge, USA

Fig. 1 MRCM simulation domains. (a) Topography (unit: m) and (b) population density (unit: persons per square kilometre; CIESIN, 2018). Blue dashed line in (a) indicates the Nile River. Red crosses in (a) denote the location of 16 weather stations in East Africa for the use of daily maximum temperature, daily mean dew point temperature, and surface pressure. Red crosses and circles in (b) indicate two stream flow gauge stations and five precipitation stations, respectively



the main focus of this paper. These countries have recently experienced an upward trend as well as increasing variability in rainfall, leading to more frequent floods and droughts (Masih et al. 2014; Siam and Eltahir 2017; Gebrechorkos et al. 2019). For example, a heavy rainfall event in 2019 with severe flooding affected an estimated 2.8 million people across the region (Wainwright et al. 2021a). Without aggressive mitigation efforts, the increasing population in East Africa will face a severe climate crisis in the next few decades. Thus, it is necessary to produce reliable near-term climate change projections to help policymakers design effective and well-informed adaptation policies.

Simulating the East African climate is, however, a great challenge for Global Climate Models (GCMs) due to the region's complex topography and diverse climate conditions, ranging from semi-arid to tropical monsoon (Flato

et al. 2013). Indeed, most state-of-the-art global climate models in the CMIP archive tend to exhibit significant systematic errors in their representation of the climate system in East Africa (e.g., Daron 2014; Ayugi et al. 2021; Wainwright et al. 2021b). These errors could be caused by several factors, such as coarse spatial resolution and inadequate representation of physical processes (Seneviratne et al. 2012; Flato et al. 2013; Im et al. 2017b; Finney et al. 2019; Finney et al. 2020; Wainwright et al. 2021b), deficiencies in simulating the African monsoon (McSweeney et al. 2015), and poor representation of ENSO and its teleconnection to Africa (Rowell 2013). Indeed, future climate projections using GCMs provide insufficient evidence for the change in rainfall in this region (Conway and Schipper 2011; Park et al. 2015; Daron 2014; Nangombe et al. 2018; Bichet et al. 2020). These substantial uncertainties make it difficult to

determine the impacts of climate change which are needed to inform and support the development of sound adaptation strategies.

In contrast, Regional Climate Models (RCMs), with finer resolution and adequate representation of physical processes, can mitigate the known problems in GCMs (Giorgi et al. 2009; Giorgi and Gutowski 2015). Thus, RCMs are appropriate tools for assessing regional climate change for a region with complex topography and land use distribution, like Africa (e.g., Laprise et al. 2013; Im et al. 2014; Alter et al. 2015; Giorgi and Gutowski 2015; Im and Eltahir 2018a). Recent studies through the Coordinated Regional Downscaling Experiment for Africa (CORDEX–AFRICA) have constructed regional climate change information for a pan-Africa domain. However, their horizontal resolution (50 km) still has limitations for use in climate impact studies.

So far, most climate change studies over East Africa using RCMs confine their attention to the end of the 21st century (2071–2100), or to a specific period in which the global mean temperature rises by 1.5 °C or 2 °C above pre-industrial levels (e.g., Dosio 2017; Déqué et al. 2017; Osima et al. 2018; Nikulin et al. 2018; Dunning et al. 2018). Moreover, only a few studies have attempted to examine the anthropogenic influences on weather extremes, such as heavy rainfall and heatwaves in the near-term future (Russo et al. 2016). Existing studies of heatwaves are primarily based on maximum temperature and do not consider the humidity effect (Engelbrecht et al. 2015; Russo et al. 2016; Dosio 2017), while heat stress impacts are significantly mediated by humidity (Pal and Eltahir 2016; Im et al. 2017a). This study considers CMIP5 GCMs, CMIP6 GCMs, and the MIT Regional Climate Model (MRCM; Pal and Eltahir 2016) to project near-term climate change and its impacts on heat stress and rainfall over East Africa.

2 Materials and methods

2.1 Data collection

In-situ rainfall measurements at Addis Ababa, Debre Markos, Dessie, Gondar, and Nekemet from the Global Historical Climatology Network (GHCN; Peterson and Vose 1997) (Fig. 1b) are used to elucidate recent trends in rainfall in the Upper Blue Nile basin. In-situ runoff data at Diem and Atbara stations (Fig. 1b) are provided through personal communications with the ministries of water in the countries of the Nile basin. Various gridded precipitation datasets are obtained from the Climate Research Unit product (CRU; Harris et al. 2020), the Global Precipitation Climatology Project (GPCP; Adler et al. 2003), the Integrated

Multi-Satellite Retrievals for the Global Precipitation Measurement mission (Huffman et al. 2019), the Tropical Rainfall Measuring Mission (TRMM; Huffman et al. 2007), and the Climate Hazards Group InfraRed Precipitation with Station (CHIRPS; Funk et al. 2015).

Dry-bulb temperature (T), dew point temperature, and surface pressure data are taken from the ERA5 reanalysis (Hersbach et al. 2020) at 3-hour intervals on $0.25^\circ \times 0.25^\circ$ horizontal resolution for the period 1976–2019. Daily mean and maximum wet-bulb temperatures (TW and TWmax) (Davies-Jones 2008) are calculated using the ERA5 data. To quantify level of human exposure to extreme heat, the categories of heat stress, defined by the US National Weather Service (USNWS), are applied. Note that a wet-bulb temperature of 31 °C, sustained for 6 h, is assumed for an extreme danger threshold of humid heat stress for various regions (Im et al. 2017a; Im et al. 2018; Choi et al. 2021).

2.2 Selection of gridded precipitation data

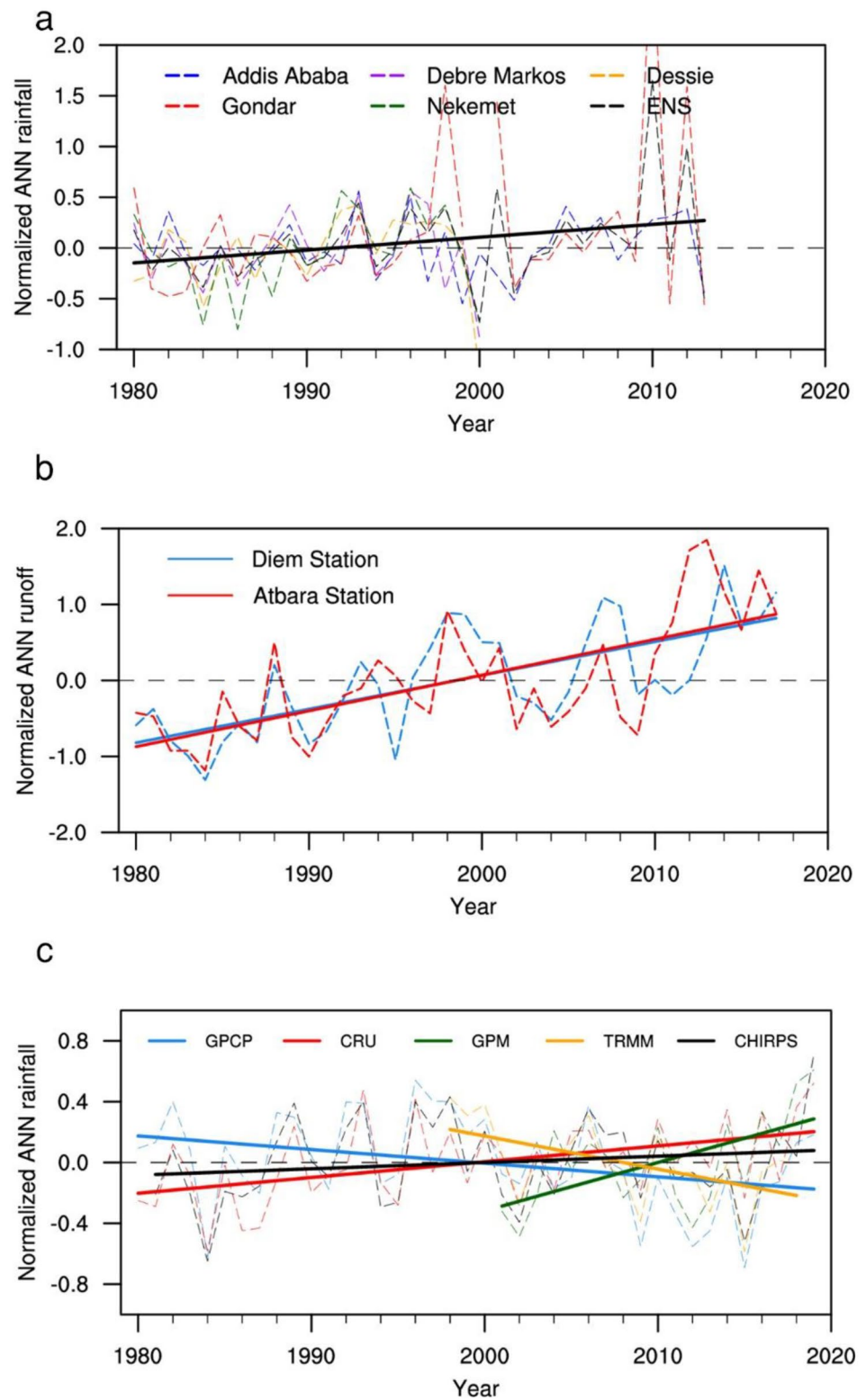
It is important to use accurate estimates of precipitation to assess the model performance and ultimately provide more reliable climate change projections. However, gridded precipitation datasets have limitations due to quality issues (Alaminie et al. 2021), especially in African countries where observational sites are spatially sparse (Sun et al. 2018).

To select a gridded precipitation data set with the best quality standards for East Africa, various precipitation estimates are compared to the in-situ observational data which provide relatively accurate measurements (Fig. 2). The decision on data selection is based primarily on its ability to represent recent climate trends. In modern records, precipitation at five stations in the Upper Blue Nile basin shows an overall increasing trend (Fig. 2a), consistent with the finding of Siam and Eltahir (2017). In addition, runoff at Diem and Atbara stations supports these rainfall trends over the region (Fig. 2b). Contrary to the observed trends, drying trends are evident in two precipitation estimates, including GPCP and TRMM (Fig. 2c). By contrast, the CRU, GPM and CHIRPS data exhibit similar trends to the in-situ observations (Fig. 2c). The CHIRPS, which has a 0.05° resolution and exhibits trends consistent with those of the station observations, is mainly used to evaluate climate simulations rather than CRU (which has a coarser spatial resolution ($0.5^\circ \times 0.5^\circ$)) and GPM (which is limited to a relatively short period (2001–2019)).

2.3 Selecting GCMs for downscaling over East Africa

As is well known from previous observational and modeling studies, the signal of anthropogenic climate change was detected in recent decades (e.g., IPCC 2013). In particular,

Fig. 2 (a) Time series of annual mean (ANN) rainfall derived from five weather stations (Addis Ababa, Debre Markos, Dessie, Gondar, and Nekemet) in the upper Blue Nile basin. (b) Time series of runoff at Diem and Atbara stations. (c) Same as (a), but for ANN rainfall averaged over the five stations derived from GPCP, CRU, GPM, TRMM and CHIRPS. Black dashed line in (a) denotes ensemble mean (ENS) of observed rainfall at five stations. All values are normalized by corresponding climatological monthly mean values. Linear trends are indicated by thick solid lines



the Sahel zone of Sudan and northern parts of Ethiopia have experienced notable climatic shift from dry to wetter conditions since the 1980s (Fig. 2), primarily due to escalating greenhouse gas emissions (e.g., Dong and Sutton 2015;

Park et al., 2016; Giannini and Kaplan 2019). This suggests that GCMs, which reasonably well simulate not only climatic conditions but also recent climate-change trends, can provide reliable future climate projections.

However, most existing studies have placed emphasis on the ability of a GCM to describe the climatological mean features (Baek et al. 2013; McSweeney et al. 2015). In this study, among the many options in the CMIP5/CMIP6 data archive, a set of 6 GCMs (three from the CMIP5 archive and three from the CMIP6 archive) are carefully selected through a rigorous screening process. We mainly consider the model's ability in capturing not only average climatic conditions, but also recent climate trends in East Africa.

To avoid duplicating existing efforts, the selection process for CMIP5 GCMs relied on previous assessment performed by McSweeney et al. (2015). We, followed their suggestion, first select six CMIP5 GCMs (GFDL-CM3, HadGEM2-ES, NorESM1-M, ACCESS1-0, MPI-ESM-MR,

and CNRM-CM5) judged to be satisfactory in their representation of key aspects of the African climate (i.e., African monsoon circulation, climatological annual cycles of temperature and precipitation, the influence of teleconnection patterns, such as El Niño –Southern Oscillation and the Indian Ocean Dipole). Among the six models, we then identify that MRCM driven by three models (GFDL-CM3, HadGEM2-ES, and NorESM1-M) reproduce the observed climate trends (Figs. 3, S1, and S2). Meanwhile, MRCM forced by CMIP5 GCMs, including ACCESS1-0, CNRM-CM5, and MPI-ESM-MR, perform poorly (Fig. 3) and are therefore eliminated from further analysis. As expected, climatological features are well captured by the three selected CMIP5 GCMs (Fig. S3).

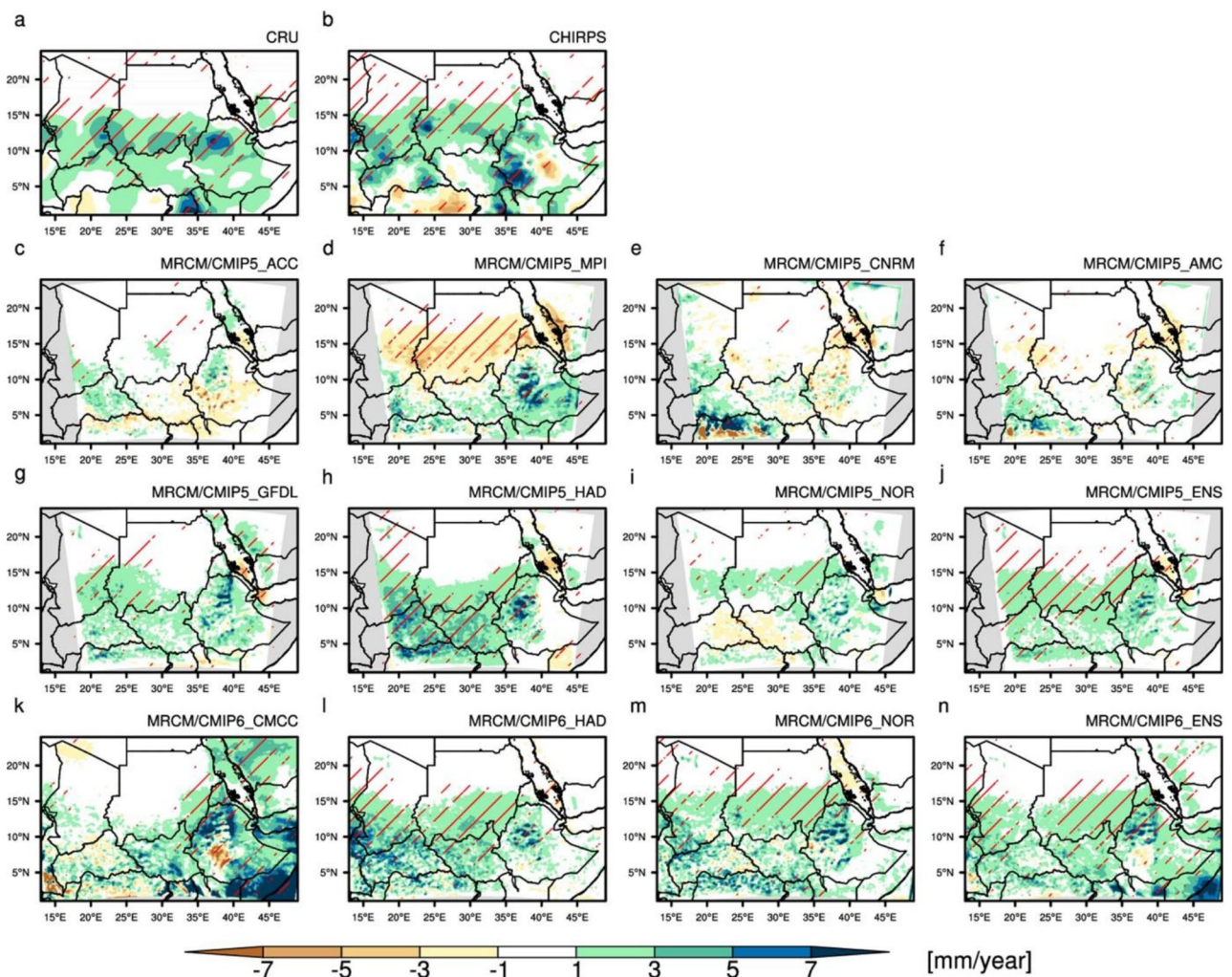


Fig. 3 Spatial distribution of historical (1976–2019) trends (unit: mm/year) in annual mean precipitation in East Africa derived from (a) CRU, (b) CHIRPS, (c–e) MRCM simulations forced by three different GCMs (ACCESS1-0 (MRCM/CMIP5_ACC), MPI-ESM-MR (MRCM/CMIP5_MPI), and CNRM-CM5 (MRCM/CMIP5_CNRM) from the CMIP5 archive), and (f) ensemble mean of the three MRCM simulations (MRCM/CMIP5_AMC). (g–j) Same as (c–f), but for GFDL-CM3

(MRCM/CMIP5_GFDL), HadGEM2-ES (MRCM/CMIP5_HAD), and NorESM1-M (MRCM/CMIP5_NOR) from the CMIP5 archive. (k–n) Same as (c–f), but for CMCC-ESM2 (MRCM/CMIP6_CMCC), HadGEM3-GC31-MM (MRCM/CMIP6_HAD), and NorESM2-MM (MRCM/CMIP6_NOR) from the CMIP6 archive. Superimposed hatching indicates regions where trends are statistically significant at the 95% confidence level based on a nonparametric Mann-Kendall test

For a selection of CMIP6 GCMs, we first select 7 GCMs among 29 GCMs by excluding 15 models with relatively coarser resolution (larger than 1.25°; Table S1) and 7 models which do not provide six-hourly SSP5-8.5 scenario data. Among the selected 7 CMIP6 GCMs, we finally select three CMIP6 GCMs (CMCC-ESM2, HadGEM3-GC31-MM, and NorESM2-MM), which show the highest Taylor skill score (Fig. S4; Taylor 2001) and reproduce the climatological features as well (Figs. 3, S1, S2, and S3).

The six GCMs (CMIP5 GCMs: GFDL-CM3, HadGEM2-ES, and NorESM1-M; CMIP6 GCMs: CMCC-ESM2, HadGEM3-GC31-MM, and NorESM2-MM) are finally selected in this study to specify the boundary conditions for MRCM. It is worth noting that the MRCM ensembles outperform most individual simulations due to the cancellation of some systematic biases.

2.4 Regional climate model and experimental setup

The MRCM is a three-dimensional hydrostatic numerical model, of which general structure and dynamical core are rooted in the International Center for Theoretical Physics (ICTP) Regional Climate Model version 3 (RegCM3; Pal et al. 2007). MRCM is notably coupled with the Integrated Biosphere Simulator land surface scheme (IBIS; Foley et al. 1996; Winter et al. 2009) and employs significant enhancements of model physics (Marcella 2012; Marcella and Eltahir 2012; Gianotti 2012; Gianotti and Eltahir 2014a, 2014b). The latest version of MRCM well represents land surface processes and has sufficient skill to simulate the fine-scale structure of climatic variables over various domains, such as North America (Winter et al. 2009), West Africa (Im et al. 2014; Im and Eltahir 2018a), Southwest Asia (Pal and Eltahir 2016; Choi and Eltahir 2022a, 2022b), South Asia (Im et al. 2017a; Choi et al. 2021), and the Maritime Continent (Im and Eltahir 2018b).

The model domain cover East Africa on a Lambert conformal projection (Fig. 1a). Note that the domain for the MRCM simulations driven by Coupled Model Inter-comparison

Project Phase 5 (CMIP5) GCMs is smaller than that for the MRCM simulations forced by CMIP6 GCMs. The horizontal resolution is 20 km in both longitudinal and latitudinal directions. As explained above, to specify the boundary conditions for MRCM, we carefully select three GCMs (GFDL-CM3, HadGEM2-ES, and NorESM1-M) from the CMIP5 archive and three GCMs (CMCC-ESM2, HadGEM3-GC31-MM, and NorESM2-MM) from the CMIP6 archive (see Sect. 2.3). We perform two 30-year time slice simulations. The first one starts in 1975 and the second time slice experiment starts in 2020. For the MRCM simulations driven by CMIP5 GCMs, time-lagged ensemble members are produced with different starting dates (i.e., January 1st, 2nd, and 3rd in 1975, and January 1st, 2nd, and 3rd in 2020) (Table 1).

To provide more reliable climate projections, it is required to eliminate systematic biases in the MRCM output. Following previous studies (Li et al. 2010; Choi et al. 2021), we apply the equidistant quantile-mapping bias correction procedure under the assumption that the bias does not change over time. Compared to the widely used quantile-mapping technique, this method explicitly considers changes in distribution between reference and projection periods. The ERA5 and CHIRPS data, which are regarded as relatively unbiased, are used to correct the bias in simulated monthly mean temperatures and precipitation (PR) over the entire domain, respectively. To correct the systematic bias apparent in model simulations at the station scale, we consider daily maximum dry-bulb temperature, dewpoint temperature, and surface pressure data derived from the GHCN at 16 stations (i.e., large population centers in Sudan and Ethiopia; Fig. 1) over East Africa. However, precipitation data over these stations are of limited use due to a large number of missing values. Thus, CHIRPS is applied to correct the precipitation bias at the 16 stations.

Table 1 Description of MRCM experiments

Experiment	Boundary conditions	Variant label	Resolution (lon × lat)	Scenario	Time-lagged ensemble members
MRCM/CMIP5_ACC	ACCESS1-0/CMIP5	rlilpl	158 × 127	historical	3
MRCM/CMIP5_MPI	MPI-ESM-MR/CMIP5	rlilpl	158 × 127	historical	3
MRCM/CMIP5_CNRM	CNRM-CM5/CMIP5	rlilpl	158 × 127	historical	3
MRCM/CMIP5_GFDL	GFDL-CM3/CMIP5	rlilpl	158 × 127	historical/RCP8.5	3
MRCM/CMIP5_HAD	HadGEM2-ES/CMIP5	rlilpl	158 × 127	historical/RCP8.5	3
MRCM/CMIP5_NOR	NorESM1-M/CMIP5	rlilpl	158 × 127	historical/RCP8.5	3
MRCM/CMIP6_CMCC	CMCC-ESM2/CMIP6	rlilplf1	214 × 139	historical/ssp5-8.5	1
MRCM/CMIP6_HAD	HadGEM3-GC31-MM/CMIP6	rlilplf3	214 × 139	historical/ssp5-8.5	1
MRCM/CMIP6_NOR	NorESM2-MM/CMIP6	rlilplf1	214 × 139	historical/ssp5-8.5	1

3 Results

3.1 Evaluation of the historical simulations

The performance of MRCM/CMIP6 is superior overall compared to the GCMs and MRCM/CMIP5 in capturing the present climate conditions over East Africa (Fig. 4, S2, and S3). Figure 4 shows the spatial distribution of annual mean PR, T, and TW derived from the observations and MRCM ensembles. In the observational record, this region has diverse climate conditions from semi-arid in the north to tropical monsoon in the south (Fig. 4a). Also, a significant temperature gradient exists between cold regions in the highlands of Ethiopia and warm regions in the lowlands of southeastern Sudan (Fig. 4d, g). These observed features are well captured by MRCM/CMIP5 and MRCM/CMIP6, despite of noticeable biases in some regions. Compared to the precipitation observations, both the MRCM ensembles

exhibit dry and wet biases in South Sudan and the highlands of Ethiopia, respectively. For dry-bulb temperature, the warm bias appears in the vicinity of South Sudan (possibly due to the lack of representation of swamps), while the cold bias is evident in the lowlands of Ethiopia and the northern part of the study area. Consistent with these cold biases, there is a significant underestimation of TW over Sudan and the lowlands of Ethiopia. Relative to MRCM/CMIP5, such structural biases are greatly reduced in MRCM/CMIP6, which could be due to the remarkable improvements in CMIP6 models (e.g., spatial resolution, physical processes, and biogeochemical cycles; Eyring et al. 2016). It is also noticeable that MRCM/CMIP6 overall shows better performance in representing the seasonal cycles of PR, T, and TW in East Africa, than GCMs and MRCM/CMIP5 (Fig. S3).

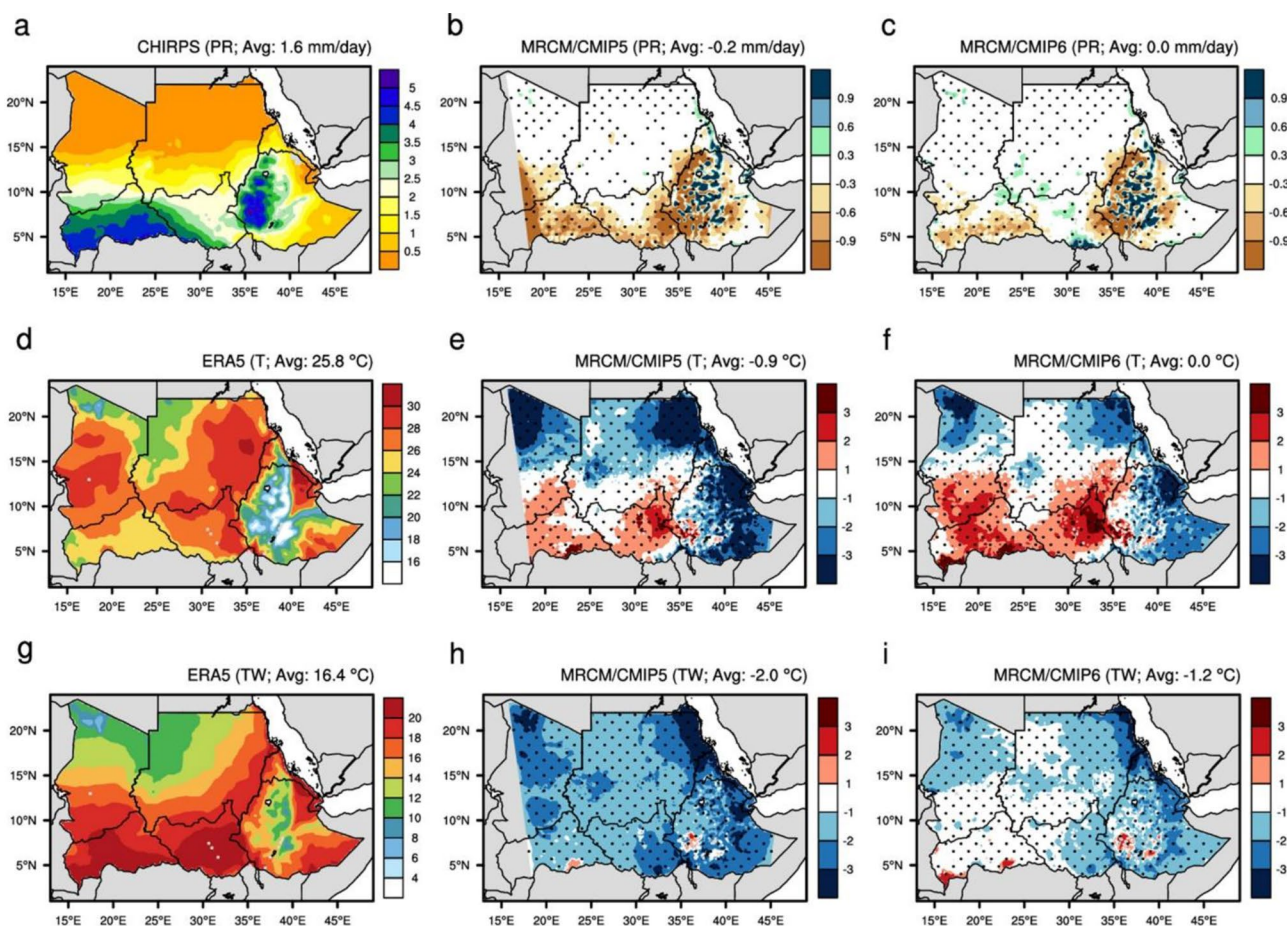


Fig. 4 (a) 30-year (1976–2005) climatology of annual mean precipitation (PR; mm/day). Differences (b) between ensemble mean of MRCM simulations driven by three CMIP5 GCMs (MRCM/CMIP5) and observation and (c) between ensemble mean of MRCM simulations driven by three CMIP6 GCMs (MRCM/CMIP6) and observation. (d–f) Same as (a–c), but for dry-bulb temperature (T; °C). (g–i) Same as (a–c),

but for wet-bulb temperature (TW; °C). Observations are interpolated to each MRCM grid. Stippling indicates regions where the differences are statistically significant at the 5% level as determined by a two-sided Student's t-test. Area-averaged value (Avg) over land (3–23°N / 19–44°E) is given on the top right corner of each plot

3.2 Projected changes in near-term temperature

MRCM ensemble projections (MRCM/CMIP5 and MRCM/CMIP6) show significant warming in East Africa with a higher inter-model agreement. Figures 5 and 6 present the projected change in T and TW by the middle of the 21st century (2021–2050) under high-emissions scenarios (RCP8.5 and SSP5-8.5). These changes are, to a large degree, spatially uniform. The overall increases in T are evident across all simulations with a slightly greater increase in arid regions of Sudan (above 2.0 °C; Fig. 5l, x). The change in T can lead to a substantial rise in TW (approximately 1.4 °C in MRCM/CMIP5 and 1.3 °C in MRCM/CMIP6). The more than 1.0 °C increase in TW is expected to increase the level of heat stress over the southeastern border of Sudan and the lowlands of Ethiopia where humid heat stress is already high in the current climate (Fig. 6). Although all MRCM simulations consistently predict the increase (more than 1.0 °C) in TW in Ethiopia, the projected TW over a mountainous region (elevation higher than 1500 m) is much lower than the USNWS extreme danger threshold of 31 °C for the future climate.

A substantial increase in daily maximum temperature (Tmax) is likely to occur in the near future (Fig. S5), along with more frequent and severe temperature extremes in East Africa (Figs. S6 and S7). Fig. S5 shows the projected changes in the annual cycle of Tmax for major cities in the study region. MRCM/CMIP6 projected that the high values of Tmax approaching 45 °C mostly appear in central and eastern Sudan, including Port Sudan, Dongola, Atbara, Khartoum, Kassala, and Gedaref in the near future. By contrast, temperature extremes in Ethiopia will remain much below the levels of Sudan, despite the substantial increase in Tmax. Overall, these increases are not confined to a particular region and season (i.e., homogeneous warming), which implies that there would not be a significant change in the seasonality of extreme temperatures. Similar results are obtained with MRCM/CMIP5. It is important to note that the increases in Tmax would not necessarily result in a proportional increase in humid heat stress, since the high risk of heat stress is not just a function of temperature, but a combined consequence of temperature and humidity (Sherwood and Huber 2010; Pal and Eltahir 2016; Im et al. 2017a; Kang and Eltahir 2018).

The MRCM ensembles project that most regions at low elevations in East Africa are expected to be susceptible to humid heat extremes, as global warming progresses (Fig. 7). In the current climate, TWmax exceeding the extreme danger threshold of 31 °C is rarely observed. Based on MRCM/CMIP6, the low elevation regions (Port Sudan, Atbara, Khartoum, Kassala, Gedaref, El Obeid, Nyala, and Gode) are expected to be exposed to frequent heatwaves with a

TWmax approaching or exceeding the USNWS extreme danger threshold of 31 °C by the middle of the 21st century under SSP5-8.5 scenario. Notably, Port Sudan, a city close to the Red sea, stands out due to its high TWmax values which are well above 31 °C and close to a human survivability threshold of 35 °C (Sherwood and Huber 2010; Pal and Eltahir 2016; Im et al. 2017a). The populous cities in Ethiopia are more likely to see a significant rise in TWmax, but the projected TWmax will be far below the USNWS extreme danger level, except for Gode. Though the projected risk of extreme heat stress will be generally lower in MRCM/CMIP6 than in MRCM/CMIP5, there is a robust inter-model consistency across different generations of models (Figs. 7 and S8).

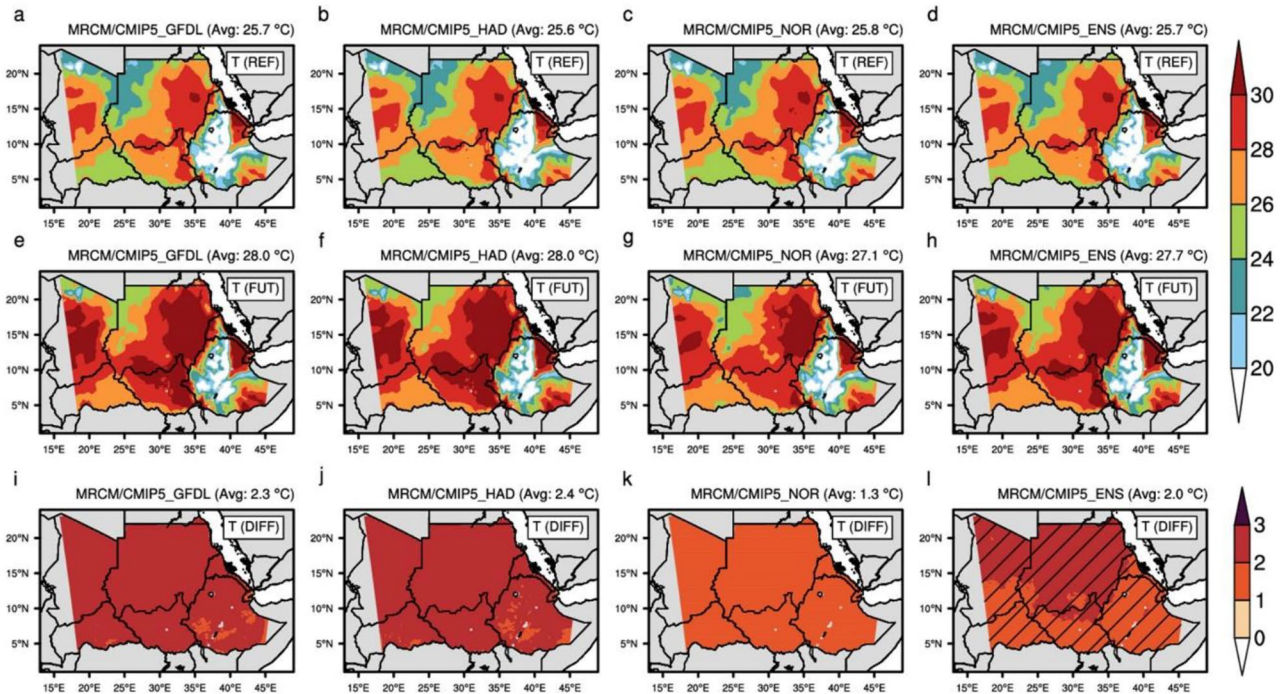
The return period analysis further confirms the elevated risks of heat stress in a warmer world (Fig. S9). For the historical period, a recurrent period of extreme heat events (above the extreme danger threshold of 31 °C) is close to or far longer than 100 years, depending on the given region. Though some discrepancy exists in different generations of CMIP experiments, significant decreases in the return period are consistently expected among different high-emissions scenarios (RCP8.5 and SSP5-8.5). For instance, extreme heat events would occur once in less than 50 years over two major cities (Port Sudan and El Obeid) in Sudan in the near-term future. In particular, the most vulnerable city to heat stress is Port Sudan with a recurrent period of less than 5 years.

3.3 Projected changes in near-term precipitation

Consistent with the observed trend of rainfall in recent decades (Figs. 2 and 3), near-term climate projections exhibit an overall increase in precipitation over East Africa (Fig. 8). Recent observation suggests that annual mean precipitation over the region increased by about 9% between the periods 1976–1997 and 1998–2019. Based on MRCM/CMIP6, annual mean rainfall over East Africa is projected to increase by about 7% under the SSP5-8.5 scenario (Fig. 8h). The consistency of the rainfall changes across MRCM/CMIP6 simulations is evident in Ethiopia. Similarly, MRCM/CMIP5 also projects an overall increase (more than 10%) in precipitation, especially in the Upper Blue Nile. On the other hand, there is limited inter-model agreement on the changes in precipitation over southwestern Sudan (Fig. 8h). Nevertheless, overall increases in rainfall are expected in the southern part of Sudan in most of the MRCM simulations, except MRCM simulation driven by CMCC which presents a small and insignificant decrease in precipitation.

The seasonal cycle of rainfall in Ethiopia is likely to amplify by midcentury, consistently across CMIP5, CMIP6,

CMIP5



CMIP6

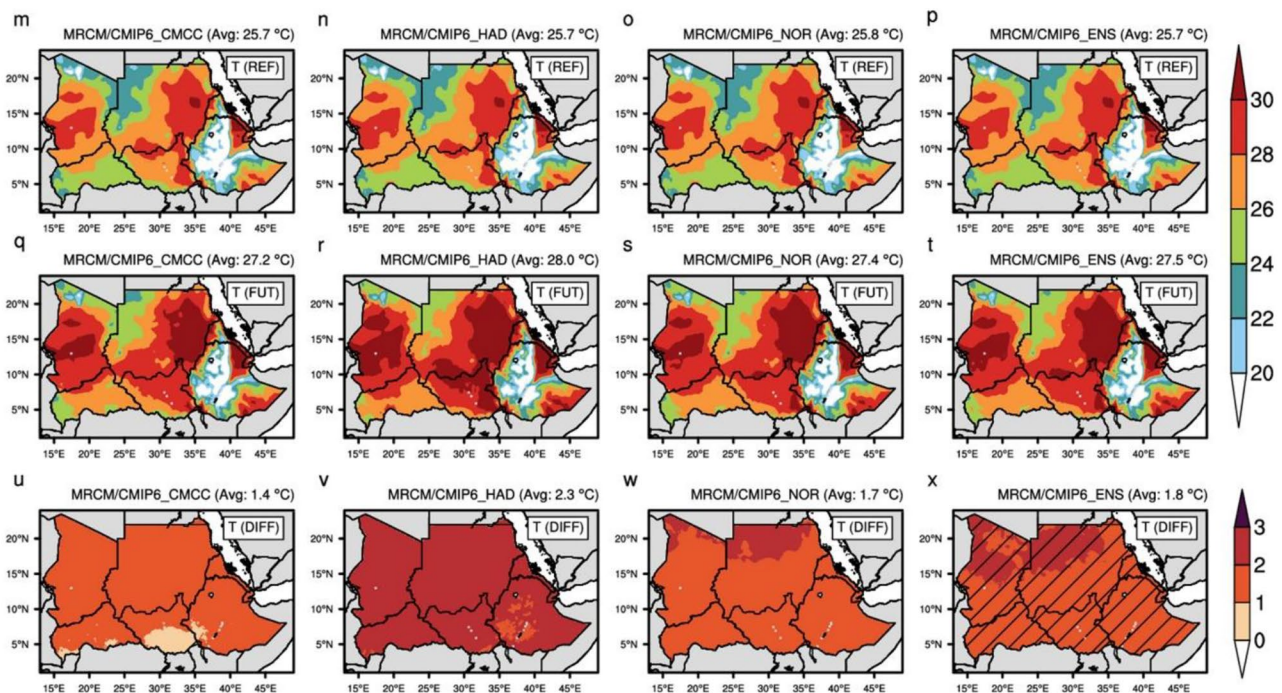
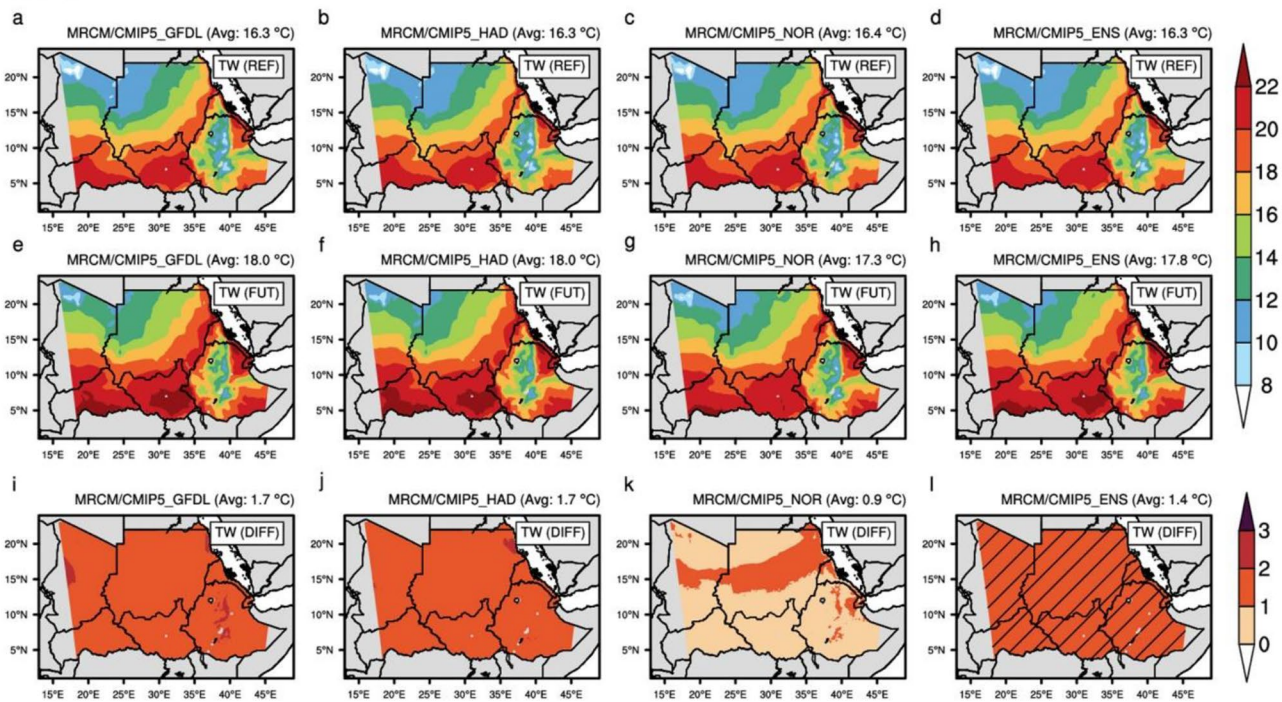


Fig. 5 Spatial distribution of annual mean dry-bulb temperature (T; unit: °C) for (a–d) reference period, (e–h) near future period, and (i–l) its change, derived from bias-corrected MRCM simulations forced by (a, e, and i) GFDL-CM3 (MRCM/CMIP5_GFDL), (b, f, and j) HadGEM2-ES (MRCM/CMIP5_HAD), and (c, g, and k) NorESM1-M (MRCM/CMIP5_NOR) from the CMIP5 archive, and (d, h, and l) ensemble mean of the three MRCM simulations (MRCM/

CMIP5_ENS). (m–x) Same as (a–l), but for CMCC-ESM2 (MRCM/CMIP6_CMCC), HadGEM3-GC31-MM (MRCM/CMIP6_HAD), and NorESM2-MM (MRCM/CMIP6_NOR) from the CMIP6 archive. Area-averaged value (Avg) over land (3–23°N / 19–44°E) is given on the top right corner of each plot (unit: °C). Superimposed hatching indicates agreement by MRCM simulations on the sign of the change

CMIP5



CMIP6

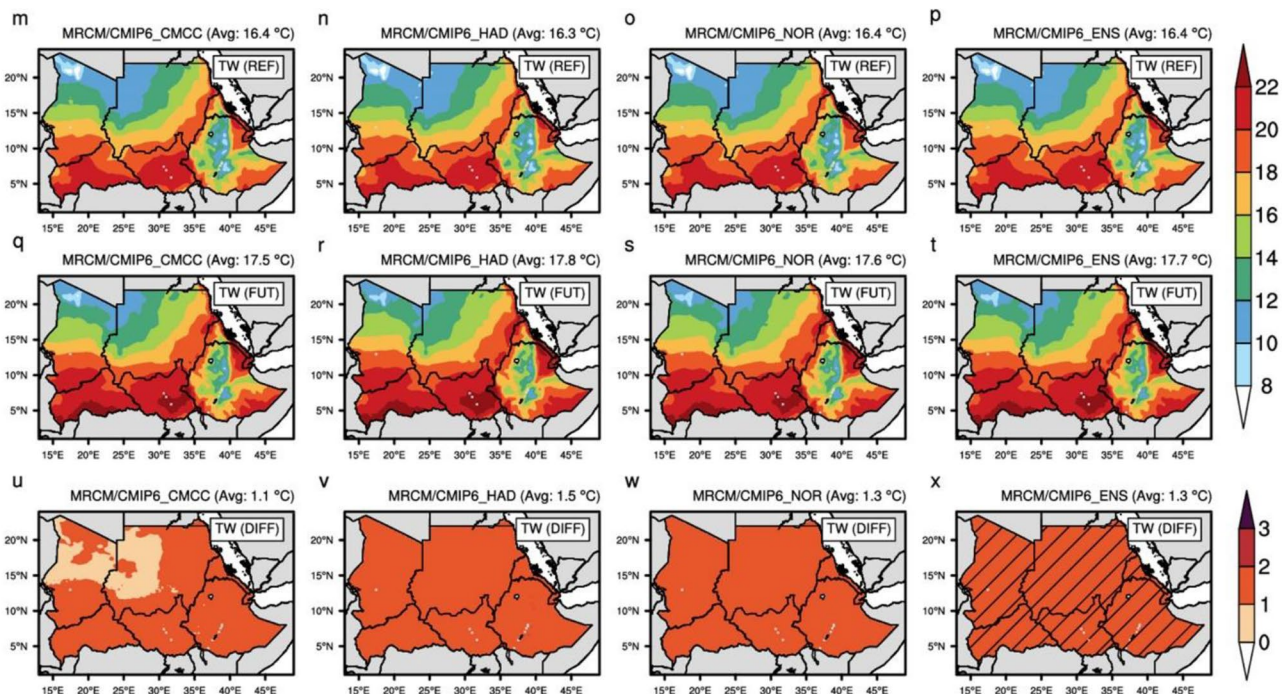


Fig. 6 Spatial distribution of annual mean wet-bulb temperature (TW; unit: °C) for (a-d) reference period, (e-h) near future period, and (i-l) its change, derived from bias-corrected MRCM simulations forced by (a, e, and i) GFDL-CM3 (MRCM/CMIP5_GFDL), (b, f, and j) HadGEM2-ES (MRCM/CMIP5_HAD), and (c, g, and k) NorESM1-M (MRCM/CMIP5_NOR) from the CMIP5 archive, and (d, h, and l) ensemble mean of the three MRCM simulations (MRCM/

CMIP5_ENS). (m-x) Same as (a-l), but for CMCC-ESM2 (MRCM/CMIP6_CMCC), HadGEM3-GC31-MM (MRCM/CMIP6_HAD), and NorESM2-MM (MRCM/CMIP6_NOR) from the CMIP6 archive. Area-averaged value (Avg) over land (3–23°N / 19–44°E) is given on the top right corner of each plot (unit: °C). Superimposed hatching indicates agreement by MRCM simulations on the sign of the change

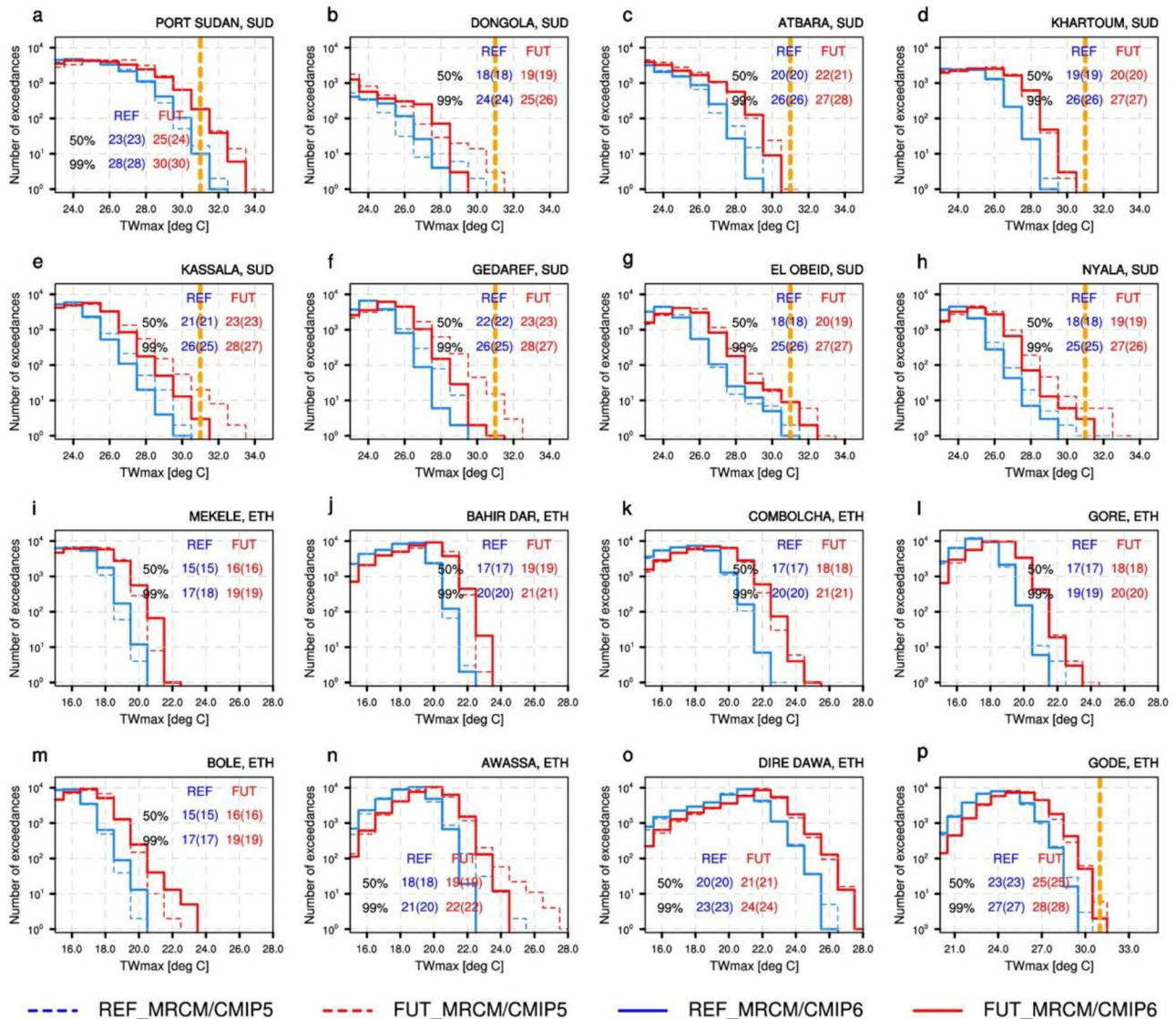


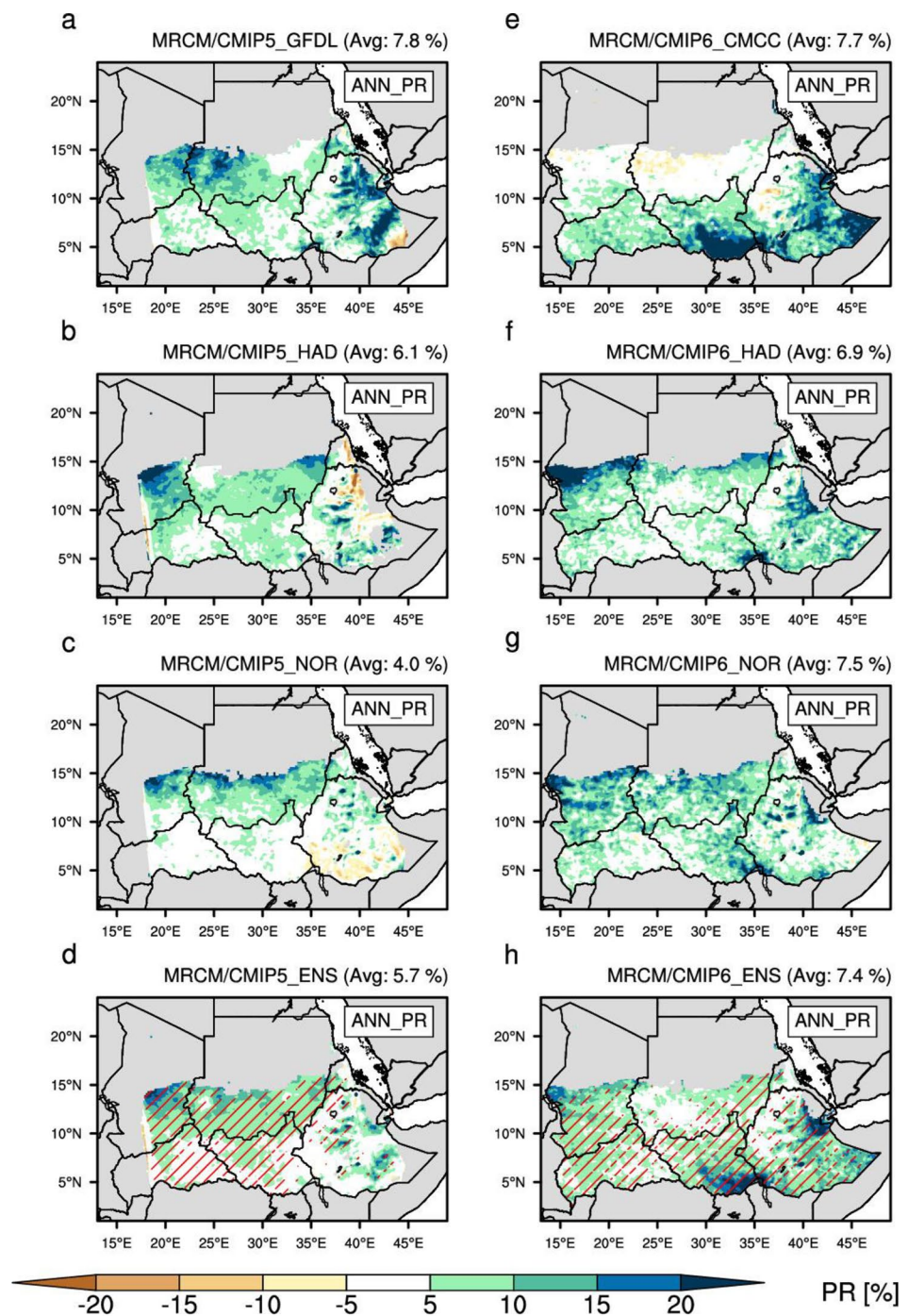
Fig. 7 Histogram of daily maximum wet-bulb temperature (TWmax; unit: °C) for sixteen major cities over East Africa derived from bias-corrected MRCM/CMIP5 under historical (REF_MRCM/CMIP5; 1976–2005) and RCP8.5 scenarios (FUT_MRCM/CMIP5; 2021–2050), and bias-corrected MRCM/CMIP6 under historical (REF_MRCM/CMIP6; 1976–2005) and SSP5-8.5 scenarios (FUT_MRCM/

CMIP6; 2021–2050). Values without parentheses represent the 50th and 99th percentile thresholds for MRCM/CMIP5. Values in parentheses is same as those without parentheses, but for MRCM/CMIP6. Vertical dashed yellow line indicates the extreme danger threshold (31 °C) defined by the U.S. National Weather Service

and MRCM simulations (Fig. 9). Figure 9 shows the projected changes in the annual cycle of PR under the high Green House Gas (GHG) emissions scenarios (RCP8.5 and SSP5-8.5). To identify the spatially heterogeneous effects of climate change, four sub-regions are considered where the precipitation response shows different behavior in climate projections (i.e., western Sudan, eastern Sudan, the highlands of Ethiopia, and the lowlands of Ethiopia). The MRCM ensembles generally project smaller precipitation changes in Sudan than GCM ensembles. Moreover, based on MRCM/CMIP6, future change in rainfall in this region is

statistically insignificant. By contrast, Ethiopia may receive significantly more precipitation (p -value < 0.05) during the late summer and autumn seasons in the middle of the 21st century. In particular, all climate projections, regardless of the CMIP phase, expect significant increases in autumn rainfall over the highlands of Ethiopia. Note that the robustness of the wetting trends across all climate simulations (CMIP5 GCMs, CMIP6 GCMs, MRCM/CMIP5, and MRCM/CMIP6) suggests the reliability of future projections in Ethiopia.

Fig. 8 Future changes in Annual (ANN) mean precipitation (PR; unit: %) with respect to present climate, derived from bias-corrected MRCM simulations forced by (a) GFDL-CM3 (MRCM/CMIP5_GFDL), (b) HadGEM2-ES (MRCM/CMIP5_HAD), and (c) NorESM1-M (MRCM/CMIP5_NOR) from the CMIP5 archive, and (d) ensemble mean of the three MRCM simulations (MRCM/CMIP5_ENS). (e-h) Same as (a-d), but for CMCC-ESM2 (MRCM/CMIP6_CMCC), HadGEM3-GC31-MM (MRCM/CMIP6_HAD), and NorESM2-MM (MRCM/CMIP6_NOR) from the CMIP6 archive. Area-averaged value (Avg) over land (3–23°N / 19–44°E) is given on the top right corner of each plot (unit: %). Superimposed hatching indicates agreement by MRCM simulations on the sign of the change. Areas with ANN total PR < 200 mm are masked out to avoid potential inflation due to small rainfall amounts



The long-term (1976–2050) trend of precipitation helps to better discern the anthropogenic climate change signal. The evolution of seasonally (September to November) averaged precipitation over the sub-regions in East Africa is shown in Fig. 10. As expected from Fig. 9, MRCM simulations show smaller precipitation changes than their GCM counterparts. The MRCM ensembles exhibit an increase in precipitation by 16 to 22% (5 to 6%) in Sudan and by 5 to 8% (12 to 17%) in Ethiopia according to the RCP8.5 (SSP5-8.5) scenario.

Large increases in precipitation with an increasing trend (p -value < 0.01) are projected to occur in the highlands of Ethiopia. The consistency between the GCM and MRCM simulations in this region is robust. It is important to note that this wetting tendency in autumn precipitation is continuously found in observations and projections, implying a century-long wetting trend that appears to be proportional to atmospheric GHG concentrations (Fig. S10).

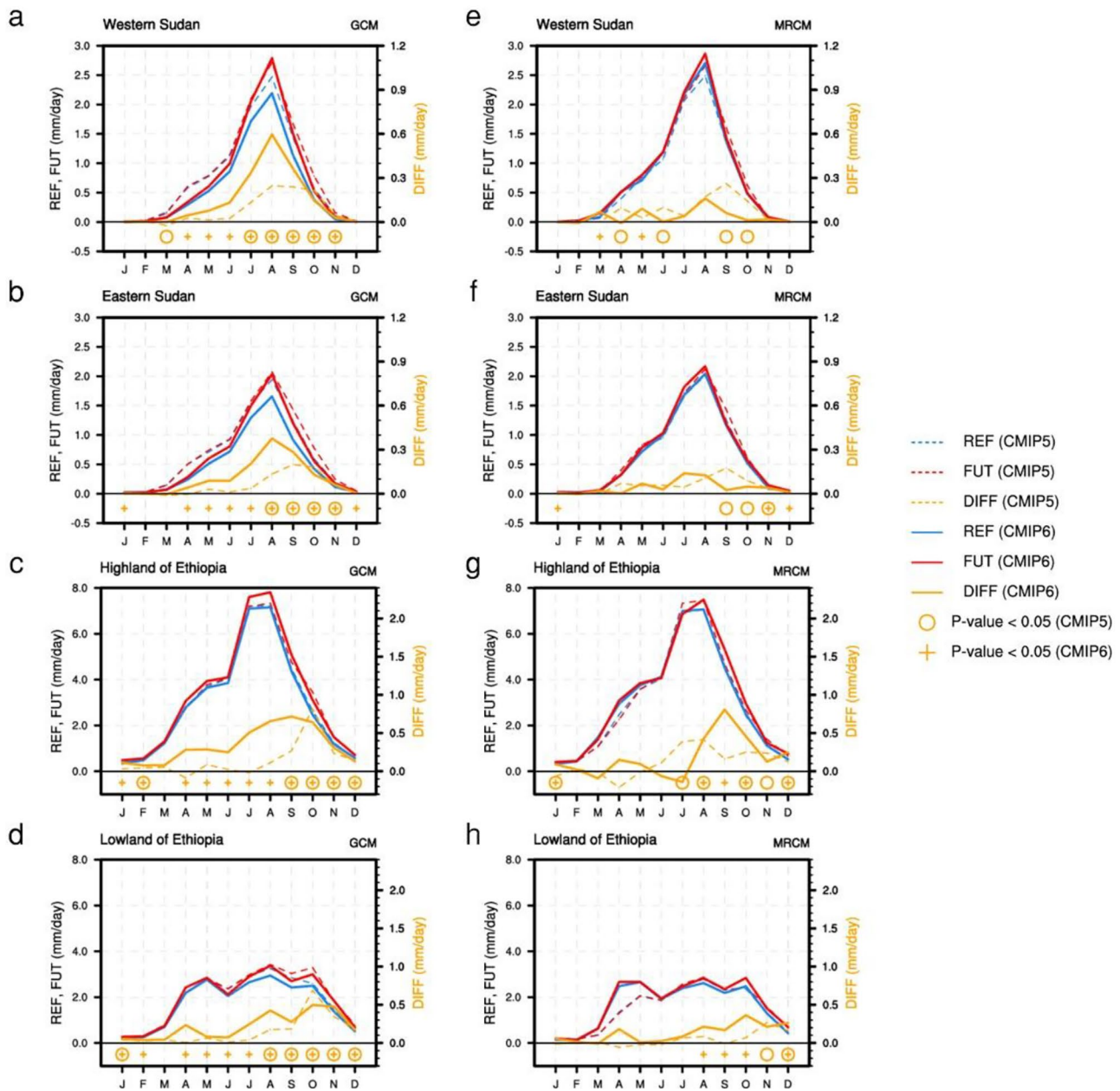


Fig. 9 The 30-year mean seasonal cycle of rainfall for four sub-regions in East Africa derived from bias-corrected ensemble means of 25 CMIP5 GCM simulations (dashed lines in a-d; see Table S1), 29 CMIP6 GCM simulations (solid lines in a-d; see Table S1), MRCM/CMIP5 (dashed lines in e-h), and MRCM/CMIP6 (solid lines in e-h)

Analyses of the return period reveal the increased risk of heavy rainfall over the next few decades in East Africa. Fig. S11 shows the return periods of annual maximum precipitation in the most populous cities over the target region. Although the return periods of extreme precipitation do not dramatically change over most regions, it overall shortens, except for Dongola, Kassala, and Combolcha. In MRCM/CMIP6 under the SSP5-8.5 scenario, a notable decrease

under historical (REF; 1976–2005) and RCP8.5/SSP5-8.5 scenarios (FUT; 2021–2050). Yellow circles (respectively plus markers) indicate the months where the rainfall change is statistically significant at the 95% confidence level in MRCM/CMIP5 (respectively MRCM/CMIP6)

of the recurrence interval appears in Port Sudan, Atbara, Nyala, Mekele, Bahir Dar, Gore, Bole, Awassa, and Dire Dawa where a 1-in-50-year extreme rainfall event in the reference climate will become an approximately 1-in-25 year event in the near future. In particular, MRCM simulations (MRCM/CMIP5 and MRCM/CMIP6) driven by CMIP5 and CMIP6 GCMs consistently project that Bahir Dar, Bole,

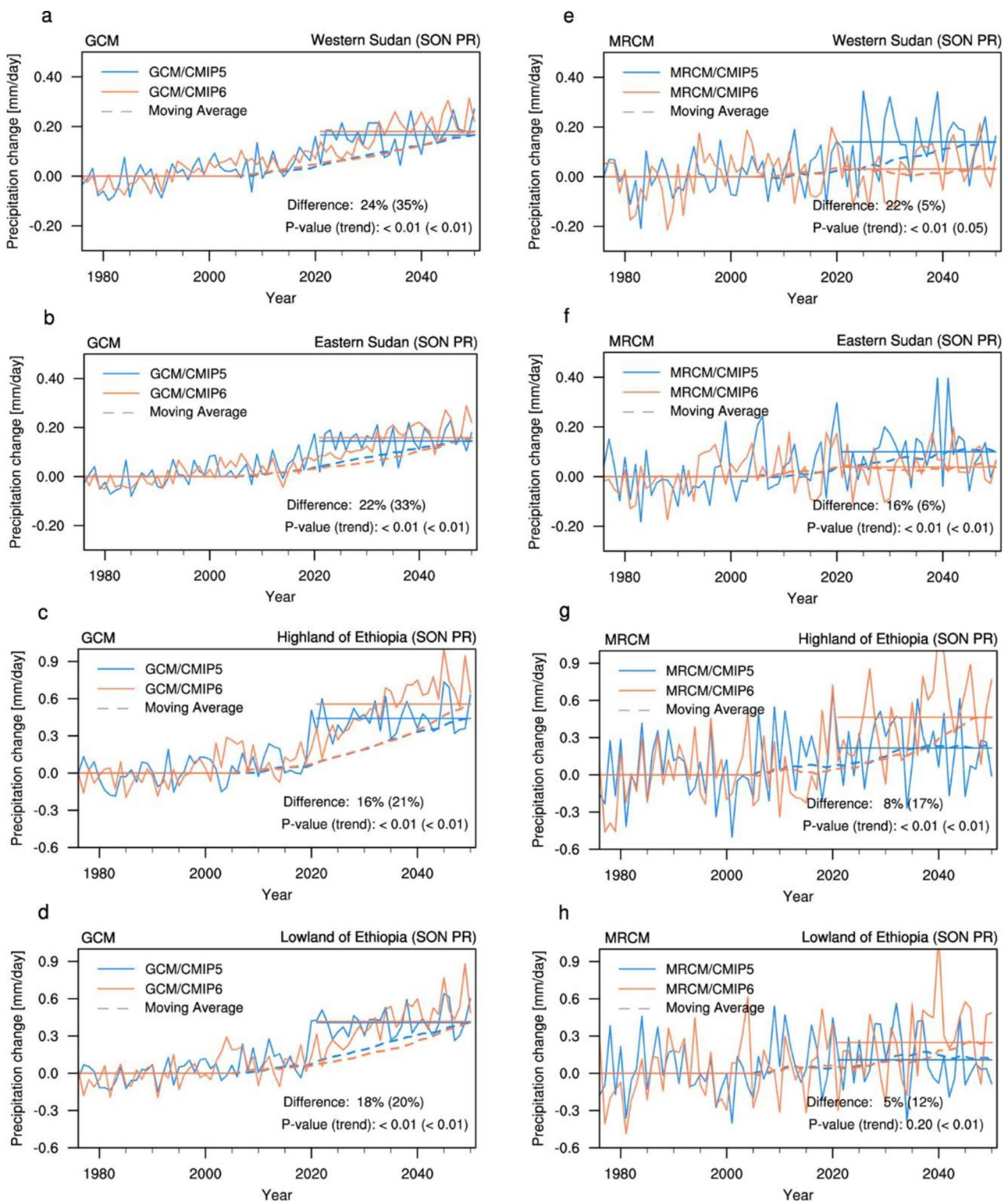


Fig. 10 Time series of seasonally (September to November; SON) averaged precipitation change in four sub-regions over East Africa for the period 1976–2050 derived from bias-corrected ensemble means of 25 CMIP5 GCM simulations (blue lines in a-d; see Table S1), 29 CMIP6 GCM simulations (red lines in a-d; see Table S1), MRCM/CMIP5 (blue lines in e-h), and MRCM/CMIP6 (red lines in e-h). Dashed lines

indicate the 30-year moving average of rainfall. Difference in each plot indicates 2021–2050 minus 1976–2005. P-value (based on a nonparametric Mann–Kendall test) for linear trend over the period 1976–2050 is located in the bottom right corner of the panel. Values without (with) parentheses in each panel are derived from MRCM/CMIP5 (MRCM/CMIP6)

and Awassa in Ethiopia will be vulnerable to extreme rainfall (Figs. S11–S12).

4 Discussion

It has recently been suggested that the most aggressive scenarios, RCP8.5/SSP5-8.5, may become increasingly implausible, while approaching the end of the 21st century, assuming significant mitigation efforts (Hausfather and Peters 2020). However, these scenarios are possible, and can still help policy makers design sound adaptation policies, particularly for the near future (Schwalma et al. 2020).

Our results are not directly comparable with the previous regional climate studies that focus on the end of the 21st century or a specific period in which the global mean temperature rises by 1.5 °C or 2 °C above pre-industrial levels. Although there are significant limitations to the comparison, our findings are broadly consistent with existing studies (Dosio 2017; Déqué et al. 2017; Osima et al. 2018; Nikulin et al. 2018; Dunning et al. 2018). For instance, based on CORDEX-Africa regional climate models, Déqué et al. (2017) investigated the consequences of a 2 °C global warming and showed that extreme heat waves become much more frequent. They also suggest that extreme precipitation could increase, although the change in rainfall is uncertain. In a similar way, Nikulin et al. (2018) and Osima et al. (2018) highlighted a pronounced summer warming and enhanced wet-season precipitation over East Africa in a warmer climate. However, contrary to our results, Mengistu et al. (2021) indicate a decrease in annual mean precipitation in the Ethiopian highlands by the end of this century, while most CORDEX-Africa models disagree on this drying trend (Dosio et al. 2019; Bichet et al. 2020).

This study naturally presents several important caveats. Although we found that CHIRPS data can capture the observed trend of rainfall in East Africa in recent decades by comparing to reliable in-situ station datasets (precipitation and runoff), caution must be taken in interpretation of the CHIRPS data as it contains some estimated values, not all true values. Complete comparison between the CMIP5 and CMIP6 scenarios is impossible because CMIP5 RCPs are different from the SSP scenarios, which contain regional forcings (land use and aerosols). For climate modeling, parameterized convection models are used in this study, which may be a source of uncertainty in the precipitation projections (Finney et al. 2019; Finney et al. 2020; Wainwright et al. 2021b). Also, regional climate projections unavoidably suffer from a significant body of uncertainties, including emission scenarios, model configurations, and regions of interest (Giorgi et al. 2009). Nevertheless, we believe that a well-validated MRCM can give reliable

near-term climate projections, though still with some systematic biases and uncertainties.

5 Summary and conclusions

Based on the high-resolution MRCM simulations, near-term climate change would significantly affect the large population centers in Sudan and Ethiopia (i.e., East Africa) under very high emissions scenarios (RCP8.5 and SSP5-8.5). The projected regional climate change features a general warming of mean temperatures with a magnitude of about 2.0 °C across the region, which further results in more frequent and severe climate extremes. We project, however, considerably heterogeneous impacts of climate change across the regions. For example, the low plain region in East Africa (Port Sudan, Atbara, Khartoum, Kassala, Gedaref, El Obeid, Nyala, and Gode) is particularly vulnerable to heat extremes in the near future with a TW_{max} approaching or exceeding the USNWS extreme danger threshold of 31 °C. Notably, the most vulnerable city to heat stress is Port Sudan, a city close to the Red sea.

In addition to the temperature increase, large population centers in East Africa are likely to experience small but significant increases in precipitation. Furthermore, all climate projections show a robust increase in autumn rainfall over the highlands of Ethiopia with more frequent and strong rainfall extremes. That is, the recurrence interval of extreme rainfall will decrease notably in Bahir Dar, Bole, and Awassa where a 1-in-50-year extreme rainfall event in the reference climate will become an approximately 1-in-25-year event in the near future under the RCP8.5/SSP5-8.5 scenario.

Our study indicates that East Africa would inevitably see exacerbated risks of extreme climate events, like dangerous heat and extreme rainfall, within a few decades without urgent climate change mitigation strategies. These heat extremes make the present semi-arid environments even harsher, contribute to food insecurity, and pose a significant public health challenge. Of particular note, most people in this region who are primarily engaged in agriculture will be vulnerable to these heatwaves. Moreover, enhanced rainfall extremes may cause severe flooding along the Blue Nile river with negative effects of agriculture. Our results identify specific regional hotspots of the near-term climate change and could help guide the development of a sound adaptation strategy.

Supplementary Information The online version contains supplementary material available at <https://doi.org/10.1007/s00382-022-06591-9>.

Acknowledgements We acknowledge the World Climate Research

Programme's Working Group on Coupled Modelling, which is responsible for CMIP, and we thank the climate modeling groups for producing and making available their model output.

Authors' contributions E.A.B.E. conceived and supervised the study. Y.W.C. performed the simulations, analyzed the output. Y.W.C., D.J.C., and E.A.B.E. contributed to the drafting and editing of the manuscript. All authors discussed the results and approved the final manuscript.

Funding Distribution Statement A: Approved for public release. Distribution is unlimited. This material is based upon work supported by the Abdul Latif Jameel Water and Food Systems Lab (J-WAFS) at MIT and the Under Secretary of Defense for Research and Engineering under Air Force Contract No. FA8702-15-D-0001. Any opinions, findings, conclusions, or recommendations expressed in this material are those of the author(s) and do not necessarily reflect the views of the Under Secretary of Defense for Research and Engineering.

Data availability All data needed to evaluate the conclusions in the paper are present in the paper. Additional data related to this paper may be requested from the authors.

Code availability All the codes are programmed by NCAR Command Language. The codes are available and maintained by Yeon-Woo Choi (choiyw@mit.edu).

Declarations

Conflicts of interest/Competing interests The authors declare no conflict of interest.

Open Access This article is licensed under a Creative Commons Attribution 4.0 International License, which permits use, sharing, adaptation, distribution and reproduction in any medium or format, as long as you give appropriate credit to the original author(s) and the source, provide a link to the Creative Commons licence, and indicate if changes were made. The images or other third party material in this article are included in the article's Creative Commons licence, unless indicated otherwise in a credit line to the material. If material is not included in the article's Creative Commons licence and your intended use is not permitted by statutory regulation or exceeds the permitted use, you will need to obtain permission directly from the copyright holder. To view a copy of this licence, visit <http://creativecommons.org/licenses/by/4.0/>.

References

- Adler RF et al (2003) The version-2 global precipitation climatology project (GPCP) monthly precipitation analysis (1979–Present). *J Hydrometeorol* 4:1147–1167
- Alaminie AA, Tilahun SA, Legesse SA, Zimale FA, Tarkegn GB, Jury MR (2021) Evaluation of Past and Future Climate Trends under CMIP6 Scenarios for the UBNB (Abay), Ethiopia. *Water* 13(15):2110
- Allam MM, Eltahir EAB (2019) Water-Energy-Food Nexus Sustainability in the Upper Blue Nile (UBN) Basin. *Front Environ Sci* 7:5
- Alter R, Im ES, Eltahir EAB (2015) Rainfall consistently enhanced around the Gezira Scheme in East Africa due to irrigation. *Nat Geosci* 8:763–767. <https://doi.org/10.1038/ngeo2514>
- Ayugi B, Zhihong J, Zhu H et al (2021) Comparison of CMIP6 and CMIP5 models in simulating mean and extreme precipitation over East Africa. *Int J Climatol* 41(15):6474–6496
- Baek HJ, Lee JH, Lee HS et al (2013) Climate change in the 21st century simulated by HadGEM2-AO under representative concentration pathways. *Asia Pac J Atmos Sci* 49(5):603–618
- Bichet A, Diedhiou A, Hingray B, Evin G, Touré N, Browne KNA, Kouadio K (2020) Assessing uncertainties in the regional projections of precipitation in CORDEX-AFRICA. *Clim Change* 162(2):583–601
- Choi YW, Campbell DJ, Aldridge JC, Eltahir EAB (2021) Near-term Regional Climate Change over Bangladesh. *Clim Dyn* 57(11):3055–3073
- Choi YW, Eltahir EAB (2022a) Uncertainty in future projections of precipitation decline over Mesopotamia. *Journal of Climate* 1–30
- Choi YW, Eltahir EAB (2022b) Heat stress during Arba'een foot-pilgrimage (World's largest gathering) projected to reach "dangerous" levels due to climate change. *Geophysical Research Letters* e2022GL099755
- CIESIN (2018) Gridded population of the world, version 4 (GPWv4): population density, Revision 11. <https://doi.org/10.7927/H49C6VHW>
- Conway D, Schipper ELF (2011) Adaptation to climate change in Africa: Challenges and opportunities identified from Ethiopia. *Glob Environ Change* 21(1):227–237
- Daron JD (2014) Regional climate messages: East Africa. In: Scientific Report from the CARIAA Adaptation at Scale in Semi-Arid Regions (ASSAR) Project. Collaborative Adaptation Research Initiative in Africa and Asia: Ottawa, ON
- Davies-Jones R (2008) An efficient and accurate method for computing the wet-bulb temperature along pseudoadiabats. *Mon Weath Rev* 136:2764–2785
- Déqué M, Calmanti S, Christensen OB et al (2017) A multi-model climate response over tropical Africa at + 2 °C. *Clim Serv* 7:87–95
- Dong B, Sutton R (2015) Dominant role of greenhouse-gas forcing in the recovery of Sahel rainfall. *Nat Clim Change* 5(8):757–760
- Dosio A (2017) Projection of temperature and heat waves for Africa under an ensemble of CORDEX Regional Climate Models. *Clim Dyn* 49(1–2):493–519. <https://doi.org/10.1007/s00382-016-3355-5fe>
- Dosio A, Jones RG, Jack C, Lennard C, Nikulin G, Hewitson B (2019) What can we know about future precipitation in Africa? Robustness, significance and added value of projections from a large ensemble of regional climate models. *Clim Dyn* 53(9):5833–5858
- Dunning CM, Black E, Allan RP (2018) Later wet seasons with more intense rainfall over Africa under future climate change. *J Clim* 31(23):9719–9738
- Eltahir EAB, Adams T, Nikiel C, Siam MS, Tuel A (2019) A path forward for sharing the Nile water: sustainable, smart, equitable, incremental. Published by the Author. ISBN: 9781734069624. Available from Amazon. <https://www.amazon.com/Path-Forward-Sharing-Nile-Water/dp/1734069619>
- Engelbrecht F, Adegoke J, Bopape MJ et al (2015) Projections of rapidly rising surface temperatures over Africa under low mitigation. *Environ Res Lett* 10:085004. <https://doi.org/10.1088/1748-9326/10/8/085004>
- Eyring V, Bony S, Meehl GA, Senior GA, Stevens B, Stouffer RJ, Taylor KE (2016) Overview of the coupled model intercomparison project phase 6 (CMIP6) experimental design and organization. *Geosci Model Dev* 9:1937–1958. <https://doi.org/10.5194/gmd-9-1937-2016>
- Finney DL, Marsham JH, Jackson LS et al (2019) Implications of improved representation of convection for the East Africa water budget using a convection-permitting model. *J Clim* 32(7):2109–2129
- Finney DL, Marsham JH, Rowell DP et al (2020) Effects of explicit convection on future projections of mesoscale circulations,

- rainfall, and rainfall extremes over Eastern Africa. *J Clim* 33(7):2701–2718
- Fischer EM, Knutti R (2015) Anthropogenic contribution to global occurrence of heavy-precipitation and high-temperature extremes. *Nat Clim Change* 5(6):560–564
- Flato G, Marotzke J, Abiodun B et al (2013) Evaluation of climate models. *Climate change 2013: the physical science basis. Contribution of working group I to the fifth assessment report of the intergovernmental panel on climate change*. Cambridge University Press, Cambridge, p 866
- Foley JA, Prentice IC, Ramankutty N et al (1996) An integrated biosphere model of land surface processes, terrestrial carbon balance, and vegetation dynamics. *Global Biogeochem Cyc* 10(4):603–628
- Funk C, Peterson P, Landsfeld M et al (2015) The climate hazards infrared precipitation with stations—a new environmental record for monitoring extremes. *Sci Data* 2:150066
- Giannini A, Kaplan A (2019) The role of aerosols and greenhouse gases in Sahel drought and recovery. *Clim Change* 152(3):449–466
- Gianotti RL (2012) Regional climate modeling over the Maritime Continent: Convective cloud and rainfall processes. Ph.D. dissertation, Massachusetts Institute of Technology, 306 pp
- Gianotti RL, Eltahir EAB (2014a) Regional climate modeling over the Maritime Continent. Part I: New parameterization for convective cloud fraction. *J Clim* 27:1488–1503
- Gianotti RL, Eltahir EAB (2014b) Regional climate modeling over the Maritime Continent. Part II: New parameterization for autoconversion of convective rainfall. *J Clim* 27:1504–1523
- Gebrechorkos SH, Hülsmann S, Bernhofer C (2019) Long-term trends in rainfall and temperature using high-resolution climate datasets in East Africa. *Sci Rep* 9:11376. <https://doi.org/10.1038/s41598-019-47933-8>
- Giorgi F, Jones C, Asrar GR et al (2009) Addressing climate information needs at the regional level: the corDEX framework. *World Meteorol Organ (WMO) Bull* 58(3):17
- Giorgi F, Gutowski WJ (2015) Regional dynamical downscaling and the CORDEX initiative. *Annu Rev Environ Resour* 40:467–490
- Harris I, Osborn TJ, Jones P et al (2020) Version 4 of the CRU TS monthly high-resolution gridded multivariate climate dataset. *Sci Data* 7:109
- Hausfather Z, Peters GP (2020) Emissions – the ‘business as usual’ story is misleading. *Nature* 577:618–620. <https://doi.org/10.1038/d41586-020-00177-3>
- Herold N, Alexander L, Green D, Donat M (2017) Greater increases in temperature extremes in low versus high income countries. *Environ Res Lett* 12(3):034007
- Hersbach H, Bell B, Berrisford P, Hirahara S, Horányi A, Muñoz-Sabater J, Nicolas J, Peubey C, Radu R, Schepers D, Simmons A, Soci C, Abdalla S, Abellan X, Balsamo G, Bechtold P, Biavati G, Bidlot J, Bonavita M, Thépaut JN (2020) The ERA5 global reanalysis. *Q J R Meteorol Soc*. <https://doi.org/10.1002/qj.3803>
- Huffman GJ, Bolvin DT, Nelkin EJ, Wolff DB, Adler RF, Gu G, Hong Y, Bowman KP, Stocker EF (2007) The TRMM multisatellite precipitation analysis (TMPA): quasi-global, multiyear, combined-sensor precipitation estimates at fine scales. *J Hydrometeorol* 8:38–55
- Huffman G, Bolvin D, Braithwaite D, Hsu K, Joyce R, Kidd C, Nelkin E, Sorooshian S, Tan J, Xie P (2019) NASA Global Precipitation Measurement (GPM) Integrated Multisatellite Retrievals for GPM (IMERG) Algorithm Theoretical Basis Document (ATBD) Version 06. NASA/GSFC, p 30
- Im ES, Gianotti RL, Eltahir EAB (2014) Improving the simulation of the West African Monsoon using the MIT regional climate model. *J Clim* 27(6):2209–2229
- Im ES, Pal JS, Eltahir EAB (2017a) Deadly heat waves projected in the densely populated agricultural regions of South Asia. *Sci Adv* 3(8):e1603322
- Im ES, Choi YW, Ahn JB (2017b) Worsening of heat stress due to global warming in South Korea based on multi-RCM ensemble projections. *J Geophys Res: Atmos* 122:11444–11461. <https://doi.org/10.1002/2017JD026731>
- Im ES, Eltahir EAB (2018a) Simulations of the observed ‘jump’ in the West African monsoon and its underlying dynamics using the MIT regional climate model. *Int J Climatol* 38(2):841–852
- Im ES, Eltahir EAB (2018b) Simulation of the diurnal variation of rainfall over the western Maritime Continent using a regional climate model. *Clim Dyn* 51:73–88
- Im ES, Kang S, Eltahir EAB (2018) Projections of rising heat stress over the western Maritime Continent from dynamically downscaled climate simulations. *Glob Planet Change* 165:160–172
- IPCC (2013) *Climate change 2013: the physical science basis. Contribution of working group I to the fifth assessment report of the intergovernmental panel on climate change*. Cambridge University Press, Cambridge, New York, p 1535
- Kang S, Eltahir EAB (2018) North China Plain threatened by deadly heatwaves due to climate change and irrigation. *Nat Commun* 9:2894. <https://doi.org/10.1038/s41467-018-05252-y>
- Kharin VV, Zwiers FW, Zhang X, Wehner M (2013) Changes in temperature and precipitation extremes in the CMIP5 ensemble. *Clim Change* 119:345–357. <https://doi.org/10.1007/s10584-013-0705-8>
- Kruger AC (2018) Africa and the Paris Agreement. *Nat Clim Change* 8(5):365–366
- Laprise R, Hernández-Díaz L, Tete K et al (2013) Climate projections over CORDEX Africa domain using the fifth-generation Canadian Regional Climate Model (CRCM5). *Clim Dyn* 41:3219–3246. <https://doi.org/10.1007/s00382-012-1651-2>
- Li H, Sheffield J, Wood EF (2010) Bias correction of monthly precipitation and temperature fields from intergovernmental panel on climate change AR4 models using equidistant quantile matching. *J Geophys Res* 115:D10
- Marcella MP (2012) Biosphere-atmosphere interactions over semi-arid regions: Modeling the role of mineral aerosols and irrigation in the regional climate system. Ph.D. dissertation, Massachusetts Institute of Technology, 282 pp
- Marcella MP, Eltahir EA (2012) Modeling the summertime climate of Southwest Asia: the role of land surface processes in shaping the climate of semiarid regions. *J Clim* 25(2):704–719
- Masih I, Maskey S, Mussá FEF, Trambauer P (2014) A review of droughts on the African continent: a geospatial and long-term perspective. *Hydrol Earth Syst Sci* 18:3635–3649. <https://doi.org/10.5194/hess-18-3635-2014>
- Meehl GA, Tebaldi C (2004) More intense, more frequent, and longer lasting heat waves in the 21st century. *Science* 305(5686):994–997
- Mengistu D, Bewket W, Dosio A, Panitz HJ (2021) Climate change impacts on water resources in the upper blue Nile (Abay) river basin, Ethiopia. *J Hydrol* 592:125614
- McSweeney CF, Jones RG, Lee RW et al (2015) Selecting CMIP5 GCMs for downscaling over multiple regions. *Clim Dyn* 44:3237–3260. <https://doi.org/10.1007/s00382-014-2418-8>
- Nangombe S, Zhou T, Zhang W, Wu B, Hu S, Zou L, Li D (2018) Record-breaking climate extremes in Africa under stabilized 1.5 °C and 2 °C global warming scenarios. *Nat Clim Change* 8:375. <https://doi.org/10.1038/s41558-018-0145-6>
- Nashwan MS, Shahid S (2019) Spatial distribution of unidirectional trends in climate and weather extremes in Nile river basin. *Theo Appl Climatol* 137:1181–1199
- Niang I, Ruppel OC, Abdrabo MA, Essel A, Lennard C, Padgham J, Urquhart P (2014) Africa. In: Barros VR, Field CB, Dokken DJ, Mastrandrea MD, Mach KJ, Bilir TE, Chatterjee M, Ebi KL,

- Estrada YO, Genova RC, Girma B, Kissel ES, Levy AN, MacCracken S, Mastrandrea PR, White LL (eds) Climate change 2014: impacts, adaptation, and vulnerability. Part B: regional aspects. Contribution of Working Group II to the Fifth Assessment Report of the Intergovernmental Panel on Climate Change. Cambridge University Press, Cambridge, pp 1199–1265
- Nikulin G, Lennard C, Dosio A et al (2018) The effects of 1.5 and 2 degrees of global warming on Africa in the CORDEX ensemble. *Environ Res Lett* 13(6):065003
- Osima S, Indasi VS, Zaroug M et al (2018) Projected climate over the Greater Horn of Africa under 1.5 C and 2 C global warming. *Environ Res Lett* 13(6):065004
- Pal JS, Giorgi F, Bi X et al (2007) Regional climate modeling for the developing world: the ICTP RegCM3 and RegCNET. *Bull Am Meteorol Soc* 88(9):1395–1409
- Pal JS, Eltahir EAB (2016) Future temperature in southwest Asia projected to exceed a threshold for human adaptability. *Nat Clim Change* 6:197–200
- Park JY, Bader J, Matei D (2015) Northern-hemispheric differential warming is the key to understanding the discrepancies in the projected Sahel rainfall. *Nat Commun* 6:5985
- Park JY, Bader J, Matei D (2016) Anthropogenic Mediterranean warming essential driver for present and future Sahel rainfall. *Nat Clim Change* 6(10):941–945
- Peterson TC, Vose RS (1997) An overview of the Global Historical Climatology Network temperature database. *Bull Am Meteorol Soc* 78:2837–2849
- Rowell DP (2013) Simulating SST teleconnections to Africa: what is the state of the art? *J Clim* 26:5397–5418
- Russo S, Marchese AF, Sillmann J, Immé G (2016) When will unusual heat waves become normal in a warming Africa? *Environ Res Lett* 11:054016. <https://doi.org/10.1088/1748-9326/11/5/054016>
- Schwalm CR, Glendon S, Duffy PB (2020) RCP8.5 tracks cumulative CO₂ emissions. *Proceedings of the National Academy of Sciences* 117(33):19656–19657
- Seneviratne SI et al (2012) Chap. 3: changes in climate extremes and their impacts on the natural physical environment. SREX. In: Field CB et al (eds) Special report on managing the risks of extreme events and disasters to advance climate change adaptation. Cambridge University Press, Cambridge, pp 109–230
- Sherwood SC, Huber M (2010) An adaptability limit to climate change due to heat stress. *Proceedings of the National Academy of Sciences* 107(21):9552–9555
- Siam MS, Eltahir EAB (2017) Climate change enhances interannual variability of the Nile river flow. *Nat Clim Change* 7(5):350–354. <https://doi.org/10.1038/nclimate3273>
- Sillmann J, Kharin V, Zwiers F et al (2013) Climate extremes indices in the CMIP5 multimodel ensemble: part 2. Future climate projections. *J Geophys Res Atmos* 118:2473–2493
- Sun Q, Miao C, Duan Q, Ashouri H, Sorooshian S, Hsu KL (2018) A review of global precipitation data sets: data sources, estimation, and intercomparisons. *Rev Geophys* 56:79–107. <https://doi.org/10.1002/2017RG000574>
- Taylor KE (2001) Summarizing multiple aspects of model performance in a single diagram. *J Geophys Res* 106:7183–7192
- Wainwright CM, Finney DL, Kilavi M, Black E, Marsham JH (2021a) Extreme rainfall in East Africa, October 2019–January 2020 and context under future climate change. *Weather* 76(1):26–31
- Wainwright CM, Marsham JH, Rowell DP, Finney DL, Black E (2021b) Future changes in seasonality in East Africa from regional simulations with explicit and parameterized convection. *J Clim* 34(4):1367–1385
- Winter JM, Pal JS, Eltahir EAB (2009) Coupling of integrated biosphere simulator to regional climate model version 3. *J Clim* 22:2743–2757
- WMO (2020) World Meteorological Organization Commission for Climatology. State of the Climate in Africa 2019. World Meteorological Organisation, Geneva. Report WMO-No.1253, 37pp

Publisher's note Springer Nature remains neutral with regard to jurisdictional claims in published maps and institutional affiliations.